Pauli quenching effects in a simple string model of quark/nuclear matter

G. Röpke and D. Blaschke

Department of Physics, Wilhelm-Pieck-Universtiy, 2500 Rostock, German Democratic Republic

H. Schulz

Central Institute for Nuclear Research, Rossendorf, 8051 Dresden, German Democratic Republic
and The Niels Bohr Institute, 2100 Copenhagen, Denmark

The method of thermodynamic Green's functions is applied to a nonrelativistic many-quark model system. A color-saturated confinement interaction is introduced by considering nearest-neighbor string configurations. The equation of state which accounts for the formation of three-particle bound states is derived within a ladder Hartree-Fock approximation. The temperature- and density-dependent energy shift of the intrinsic nucleonic system is calculated by considering the exchange symmetry (Pauli principle) between the quark constituents of the nucleons. The relation of this nucleonic quasiparticle energy shift to nuclear-matter data is pointed out. It is shown that beyond a critical density the nucleonic clusters are dissolved due to the Pauli quenching effects. The hadronic-to-quark-matter phase transition is considered at zero temperature.

I. INTRODUCTION

Although there has been considerable success in understanding the properties of hadrons on the basis of their quark substructures as derived within quantum chromodynamics (QCD), a rigorous use of QCD for multihadron systems is not yet in reach. Therefore, in order to gain insight into the new qualitative effects and to obtain finally calculable expressions, a more phenomenological approach has been established which is based on empirical quark-quark interaction potentials, cf. Refs. 1—11. The genuine quark interaction potential diverges at large distances and reflects in this way the confinement character. This property is in contradiction to the behavior of ordinary interaction potentials which in general can be adjusted in such a way that they vanish for infinite interparticle distances. Thus, being of no difficulty for bound-state quark clusters such as mesons and baryons, the treatment of a confinement potential requires some new ideas if a many-quark system is considered.

Effective nonrelativistic Hamiltonian approaches, where the confinement interaction is taken as the sum of two-body confinement potentials, have succeeded remarkably well in describing properties of single hadrons such as, for instance, the low-lying mass spectrum, magnetic properties, etc. Furthermore, the effective quark potential approach is also successfully applied to describe multihadron systems and to calculate, e.g., the deuteron form factor, the nucleon-nucleon scattering phase shifts, the effect of embedding a nucleon into nuclear matter [European Muon Collaboration (EMC) effect], and others which seem to signal the presence of the quark substructure in the hadrons. For the extended literature on these subjects the reader is referred to the recent reviews[8—11] and the references therein.

In dealing with multihadron systems, the potential model has to be modified in order to avoid unphysical ef-

fects as the color—van der Waals force between color-singlet clusters. According to Oka[10] the confinement potential for multihadron systems should satisfy the following conditions: (i) additivity of two-body confinement forces within color-singlet clusters; (ii) asymptotic separability of color-singlet clusters; and (iii) exchange symmetry among the quarks (on account of the Pauli principle). These conditions are considered within the string-flip model of Lenz et al.,[12] who formulated a nonrelativistic quantum-mechanical approach to a many-quark system.

Independently, the concept of saturation of the two-body interaction within colorless clusters was introduced, to derive a quantum-statistical approach[13] to a nonrelativistic quark potential model. One of the main tasks of quantum statistics is the evaluation of the many-body aspects within, e.g., the grand canonical ensemble, so that not only the ground-state properties of the multiquark system, but those at finite temperatures and densities can be calculated as well. Some of the important questions which can be attacked within such an approach are the behavior of hadrons embedded in nuclear matter, the phase transition from hadronic matter to quark matter, the response of the system to temperature and compression effects, and the modifications in the quark system within the nonequilibrium state.

This paper is organized in the following way. We begin our discussion in Sec. II with the introduction of the model Hamiltonian for the multiquark system. In Sec. III we derive in the spirit of the Bethe-Goldstone treatment of the many-body problem an equation of state which reflects the clustered hadronic phase as well as the free-quark phase. After having discussed the saturation of the confinement interaction in Sec. IV, a simple model calculation is represented in Sec. V for the quadratic quark confinement model potential. With the equation of state which is based on a unique description of both the clustered as well as the free-quark matter phase, the sta-

G. RÖPKE, D. BLASCHKE, AND H. SCHULZ

bility of hadronic matter and the possible hadronic-to-quark-matter transition is considered at zero temperature. More realistic parametrizations of the equation of state are considered in Sec. VI. There, the stability of nuclear matter with respect to phase separation is studied. Concluding remarks are given in Sec. VII.

II. MODEL HAMILTONIAN FOR MULTIQUARK SYSTEMS

We will briefly outline the underlying model to be employed for the calculations of the quark substructures of matter. Within a nonrelativistic potential description, the Hamiltonian for a system consisting of N quarks takes the form

$$H = \sum_{i=1}^{N} (m_i + p_i^2/2m_i) + V(\mathbf{r}_1, \ldots, \mathbf{r}_N) , \tag{1}$$

where m_i stands for the quark masses, and $p_i^2/2m_i$ is the kinetic energy. Usually, the potential energy is taken as the sum over all pair interactions:

$$V^{\text{conf}}(\mathbf{r}_1, \ldots, \mathbf{r}_N) = \sum_{i<j} V^{\text{conf}}(r_{ij}) , \tag{2}$$

where $V^{\text{conf}}(r_{ij})$ stands for the confining quark-model potential acting between two quarks. In this approximation the Hamiltonian formalism has successfully been applied to describe the properties of color-neutral clusters of three quarks (baryons) or quark-antiquark systems (mesons), cf. Refs. 3–8. However, the expression (2) for the potential energy cannot directly be applied to a many-quark system, because unphysical effects such as the color—van der Waals force and divergent total energy would arise.

To introduce a potential energy appropriate for a many-quark system (matter) we consider an ensemble consisting of an arbitrarily given color-neutral number of
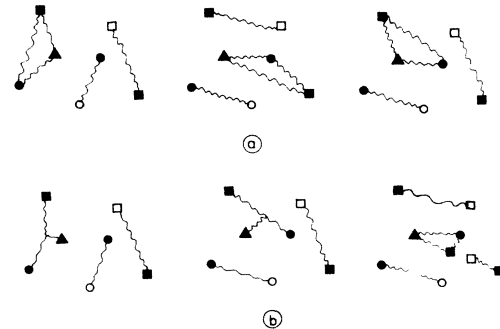

FIG. 1. (a) String configurations attributed to identical quark positions: two-body strings. (b) Three-body string and $q\bar{q}$ pair creation.

quarks and antiquarks with given net baryonic charge and make use of the adiabatic approach of Ref. 13. According to this adiabatic approach, for a given state vector $(\mathbf{r}_1, \ldots, \mathbf{r}_N)$ of the total system all possible decompositions into three quark of quark-antiquark color-singlet clusters are taken into account within a string model. The interaction potential is assigned only to those clusters whose quark constituents are interacting via strings. The resulting potential energy becomes then also a function of the string configuration

$$V^{\text{string}}(\mathbf{r}_1, \ldots, \mathbf{r}_N; \text{string configuration}) = \sum_{\text{strings}} V^{\text{conf}}(r_{ij}) . \tag{3}$$

This stringlike picture is illustrated in Fig. 1(a), where for identical quark positions possible color-singlet string configurations are depicted.

In the adiabatic approach the potential energy in (1) is associated with those string configurations which give a minimal potential energy at fixed quark positions:

$$V(\mathbf{r}_1, \ldots, \mathbf{r}_N) = \min[V^{\text{string}}(\mathbf{r}_1, \ldots, \mathbf{r}_N; \text{string configuration})] . \tag{4}$$

The phenomenological many-quark model Hamiltonian is then defined by Eq. (1) where the potential energy is calculated according to Eq. (4). Three-body string configurations as depicted in Fig. 1(b) are not considered in the present work. Furthermore, the $q\bar{q}$ pair creations [cf. Fig. 1(b)], which become essential at high temperatures and/or high densities are presently discarded. Also, color-nonsinglet clusters as discussed, e.g., by Lenz et al.[12] will not be considered here. The adiabatic approach may be improved by averaging over all possible string configurations. Such a task is beyond the scope of the present work.

We would like to stress that because of the definition of a confinement many-quark potential (4) the interaction energy is not simply given through the sum of additive pair forces as one knows from Coulomb systems, but the apparent saturation property of the quark potential

$V^{\text{conf}}(r_{ij})$ may rather be compared with the homeopolar binding within chemical compounds. The consideration of the minimal string energies (4) implies that the string interaction takes place mainly between next neighbors, and this fact permits us to avoid the rather involved problem of determining the minimal string energy configuration for given quark positions. Therefore, in the following we restrict ourselves to next-neighbor string configurations and introduce the distribution function of string lengths $c(r)$. Thus $c(r)$ defines the probability that two quarks at distance r are next neighbors (see also Sec. IV). In doing so one can replace the complicated interaction potential (4) by an effective one governed by the string length distribution function $c(r)$:

$$V^{\text{eff}}(r_{ij}) = V^{\text{conf}}(r_{ij})c(r_{ij}) . \tag{5}$$

Because of the appearance of the string length distribution $c(r)$ in Eq. (5), the resulting density-dependent effective potential is no longer divergent for large interquark separations, because $c(r)$ decreases exponentially, cf. Sec. IV.

Instead of the Hamiltonian (1) with the potential energy (4) we consider in this paper the following effective nonrelativistic Hamiltonian:

$$H^{\text{eff}} = \sum_i (m_i + p_i^2/2m_i) + \sum_{i<j} V^{\text{eff}}(r_{ij}) \ . \tag{6}$$

This form of the effective Hamiltonian has familiar properties met in many-particle physics and, therefore, can be handled by making use of the known techniques of quantum statistics. Setting formally $V^{\text{eff}} = 0$, a free-quark propagator can be introduced, and the interaction part can be treated by perturbation theory and partial summations (see the next section).

III. EQUATION OF STATE
FOR A MULTIQUARK SYSTEM

Starting with the Hamiltonian (6) and employing the usual methods of quantum statistics,[14] we derive now for the multiquark system an equation of state which considers within a unique description the clustered quark phase (nuclear matter) and the free-quark matter stage. Information about equilibrium properties of a many-particle system are contained in the correlation or Green's functions. We start with the single-particle and two-particle thermodynamic Green's functions, $G_1(1,z)$ and $G_2(12,34,z)$, where $1 = (p_1, \alpha_1)$ denotes momentum and further quantum numbers such as color, flavor, and spin, and the quantity z stands for the complex frequency variable.

The quark momentum distribution function $n(1)$, the quark-quark correlation function $\rho_{\alpha_1\alpha_2}(\mathbf{r}_1 - \mathbf{r}_2)$, and the density (equation of state) $n(\beta,\mu)$ as a function of the temperature β^{-1} and the quark chemical potential μ are then obtained according to

$$n(1) = \int \frac{d\omega}{\pi} f_{\alpha_1}(\omega) \text{Im} G_1(1, \omega + i0) \ , \tag{7}$$

$$\rho_{\alpha_1\alpha_2}(\mathbf{r}_1 - \mathbf{r}_2) = \frac{1}{-i\beta} \sum_{\Omega_\lambda} \sum_q G_2(p_1\alpha_1; p_2\alpha_2; p_1 + q, \alpha_1; p_2 - q, \alpha_2; \Omega_\lambda) \exp[-i q(\mathbf{r}_1 - \mathbf{r}_2)] \ , \tag{8}$$

$$n(\beta,\mu) = \frac{1}{\Omega} \sum_1 n(1) \ . \tag{9}$$

Here $\Omega_\lambda = 2\pi\lambda/(-i\beta) + 2\mu$ with $\lambda = 0, \pm1, \pm2, \dots$ are the two-particle Matsubara frequencies, and $f_\alpha(\omega) = [\exp\beta(\omega - \mu_\alpha) + 1]^{-1}$ is the quark Fermi distribution function. We consider a three-color model with two degenerated flavors (u,d). The contributions of antiquarks (real and virtual) will be completely dropped (however, see the remarks on the binding part of nuclear forces in Sec. V). Within this approximation scheme the baryon density n_B coincides with the density of quarks of given color and is one-third of the total quark density n, i.e., $n_B = \frac{1}{3}n(\beta,\mu)$.

Applying the Matsubara technique, the Green's functions are evaluated by perturbation expansion as described by the usual diagram notation. Following the lines of a treatment of hot nuclear matter[15] a Bethe-Goldstone–type equation arises which is equivalent to an effective wave equation for a color-singlet three-quark cluster embedded in a medium consisting of quarks which may form composites (hadrons):

$$\sum_{i=1}^3 (m_i + p_i^2/2m_i - E_{\nu P})\psi_{\nu P}(123) + \sum_{i<j}^3 \sum_{1'2'3'} V_{ij}(123,1'2'3')\psi_{\nu P}(1'2'3') = -\sum_{1'2'3'} \hat{V}(123,1'2'3')\psi_{\nu P}(1'2'3') \ . \tag{10}$$

The operator $\hat{V}$ containing the in-medium effects is usually described in diagram technique. An approximate form for it including the Pauli-blocking effects is represented in Appendix A.

We solve Eq. (10) in perturbation theory and obtain, for the three-quark cluster (nucleon) energy,

$$E_{\nu P} = E_{\nu P}^0 + \Delta E_{\nu P}^{\text{Pauli}} \ . \tag{11}$$

$E_{\nu P}^0$ is the unperturbed energy eigenvalue of the isolated three-particle cluster [left-hand side of Eq. (10)] of total momentum P and internal quantum number ν. The corresponding antisymmetrized eigenfunction is denoted by $\psi_{\nu P}^0$. The shift $\Delta E_{\nu P}^{\text{Pauli}}$ accounts for the Pauli-blocking (phase-space occupation) due to the surrounding quark composites (with distribution function $f_3(E) = [\exp\beta(E - 3\mu) + 1]^{-1}$) and possible free quarks [distribution function $f_{\alpha_1}(1)$]. As derived in Appendix A, it takes the form

$$\Delta E_{\nu P}^{\text{Pauli}} = \sum_{123} |\psi_{\nu P}(123)|^2 [E(1) + E(2) + E(3) - E_{\nu P}^0][f_{\alpha_1}(1) + f_{\alpha_2}(2) + f_{\alpha_3}(3)]$$

$$+ \sum_{123} \sum_{456} \sum_{\nu'P'} \psi_{\nu P}^*(123)\psi_{\nu'P'}(456)f_3(E_{\nu'P'}^0)\{\delta_{36}\psi_{\nu P}(123)\psi_{\nu'P'}^*(456) - \psi_{\nu P}(453)\psi_{\nu'P'}^*(126)\}$$

$$\times [E(1) + E(2) + E(3) + E(4) + E(5) + E(6) - E_{\nu P}^0 - E_{\nu'P'}^0]$$

$$= \Delta E_{\nu P}^{\text{Pauli,free}} + \Delta E_{\nu P}^{\text{Pauli,bound}} \ . \tag{12}$$

The account of the Pauli principle has the important consequence that the formation of a bound state is quenched due to the presence of surrounding free particles $(f_{\alpha_1}(1))$ giving rise to $\Delta E_{\nu P}^{\text{Pauli,free}}$ [first term on the right-hand side of Eq. (12)] and bound states $(f_3(E_{\nu P}^0))$ leading to $E_{\nu P}^{\text{Pauli,bound}}$ [second term on the right-hand side of Eq. (12)].

In Ref. 15 a similar problem has been considered: namely, the formation and destruction of bound states of nuclei as deuterons, tritons, ^{3}He and ^{4}He embeddeded in hot nuclear matter which may be produced in the course of a high-energy nucleus-nucleus collision. It is clear that the consideration of this Mott-type mechanism is also of decisive significance in describing the nucleon properties within the quark picture. Especially, when calculating the equation of state the Pauli quenching mechanism controls the destruction of bound states at high baryon densities and, therefore, it has to be one of the main ingredients of a general theory describing the transition from bound to free quarks within a unique model. But as we will see, the consideration of the Pauli-blocking effect plays already an important role in understanding the properties of hadronic matter at nuclear matter saturation density.

Notice that in (12) the Pauli principle is realized also at the nucleonic level; i.e., in the summations over $\nu'P'$ the terms $\nu=\nu'$ and $P=P'$ in the curly brackets cancel, because $P=P'$ demands $p_3=p_6$ for the quark momenta. Such a compensation is also known from the Hartree-Fock approximation and forbids the interaction of a nucleon (νP) with another nucleon in the same state. Of course, since the nucleons are not elementary particles, the underlying commutation relations for these composites are not purely fermionic but contain density corrections. However, in lowest-density order [as is the case of Eq. (12)], the fermionic character of the nucleons is retained. This is in agreement with the general scheme that composites behave in the low-density limit as elementary particles.

Applying perturbation theory,[15] the quark momentum distribution function is derived from the single-particle Green's function,

$$n(1)=f_{\alpha_1}[E(1)+\Delta(1)]$$
$$+\sum_{23}\sum_{\nu P}f_3(E_{\nu P}^0+\Delta E_{\nu P}^{\text{Pauli}})\,|\,\psi_{\nu P}(123)\,|^2\,, \quad (13)$$

and can be divided into a single-particle contribution and a bound-state contribution. In the single-particle contribution, the quantity $\Delta(1)$ is the single-particle energy shift of a quark, and in Hartree approximation it is given by

$$\Delta(1)=\sum_2 V(12,12)f_{\alpha_2}(2)\,. \quad (14)$$

The equation of state (9) is obtained from (13) by summing over the variables $1=(p_1,\alpha_1)$. Having the density $n(\mu,T)$ at our disposal, the free energy per quark f follows from

$$f(n_B,T)-f(n_B^0,T)=\frac{1}{n_B}\int_{n_B^0}^{n_B}\mu(n_B',T)dn_B' \quad (15)$$

and permits us to calculate further thermodynamical

quantities via this potential with respect to the baryon density n_B and the temperature T. Especially, at $T=0$ the free energy coincides with the internal energy $E=E_{\text{kin}}+E_{\text{pot}}$ per quark and is related to the single-particle energy shift Δ of a free-quark system according to

$$\Delta(n_B,T=0)=\frac{\partial}{\partial n_B}[n_B E_{\text{pot}}(n_B,T=0)]\,. \quad (16)$$

The approximation scheme developed in this section permits one to evaluate the quark Green's functions in such a way that the composite formation and statistical correlations (Pauli principle) can be taken into account. Therefore, we are able to study the transition from a hadronic phase, where bound-quark states dominate, to a state of free quarks within a unique picture. As we will show below, this transition is mainly controlled by the Pauli quenching mechanism. Of course, our approach allows also for more sophisticated approximations concerning the correlation function, but at present we intend to discuss the simplest nontrivial approximation which includes the new features and is of fundamental interest to develop a general theory.

IV. SATURATION OF THE CONFINEMENT INTERACTION

A main ingredient of our approach to the thermodynamical description of a confinement interaction model is the concept of saturation of the interaction within color-singlet clusters, i.e., within different cluster decompositions of a given distribution of the quark locations [see Fig. 1(a)]. The most preferable configurations are those of lowest energy of the strings. Considering the time evolution of the quark system the strings are allowed to flip from one configuration to another. The distribution of the lengths of different strings is calculated as done in Ref. 13 by utilizing the methods of statistical physics. In so doing we introduce the probability $p_{\gamma_1\gamma_2}(r_{12})$ that for a quark located at r_1 with color γ_1 the next-neighbored quark with color γ_2 is found at r_2. This concept of saturated strings is in close analogy to the quantum-mechanical treatment of the string flip model by Lenz et al.[12]

In contrast with the two-quark distribution function $\rho_{\alpha_1\alpha_2}(r_1,r_2)$ cf. Eq. (8) which represents the density of two quarks being located at $(r_1\alpha_1)$ and $(r_2\alpha_2)$, respectively, and which is normalized through

$$\int d^3r_1\int d^3r_2\rho_{\alpha_1\alpha_2}(r_1,r_2)=\tfrac{1}{16}n_B^2\Omega^2\,, \quad (17)$$

the probability $p_{\gamma_1\gamma_2}(r_{12})$ that two quarks are next neighbors is normalized to unity, i.e.,

$$\int d^3r_{12}p_{\gamma_1\gamma_2}(r_{12})=1\,. \quad (18)$$

The prefactor $\frac{1}{16}$ on the right-hand side (RHS) of Eq. (17) reflects the two-spin and two-flavor degrees of freedom.

Let us denote by $0\leq c(r)\leq 1$ the probability that a quark found at distance r from a given point is the next-neighbored one of this point. The probability distribution $c(r)$ is then determined through the integral equation

$$n(r) = n(r)c(r) + \int_{r'<r} d^3r' \rho_2(\mathbf{r}-\mathbf{r}')c(r') \ , \qquad (19)$$

where $n(r)$ is the quark density distribution and $\rho_2(\mathbf{r}-\mathbf{r}')$ is the two-particle distribution function. (At the moment internal degrees of freedom of the quarks are discarded.) The second term on the RHS of Eq. (19) takes into account that within a sphere of radius r a further particle may be found at $\mathbf{r}'$ being the next-neighbored one with respect to that at $r=0$, so that the particle located at $\mathbf{r}$ is no longer the next neighbor.

For the case of independent particles with density $n(r) = n_0 = \text{const}$ and $\rho_2(\mathbf{r}-\mathbf{r}') = n_0^2$ Eq. (19) has the solution

$$c(r) = \exp\left[-\frac{4\pi}{3} n_0 r^3 \right] \ . \qquad (20)$$

The function $p(r) = n_0 c(r)$ gives now the probability that the next neighbor is found at distance r from the reference point located at $r=0$. [Remember, that a quite analogous distribution function $p(r)$ is used in solid-state physics to describe the distribution of donor-acceptor separation in doped semiconductors.]

The probability to find a next neighbor with given color γ_2 at distance r_{12} from a quark with color γ_1 one calculates in the same way as (20). For the uncorrelated medium one obtains

$$p^{(2)}_{\gamma_1\gamma_2}(r_{12}) = n_B \exp\left[-\frac{4\pi}{3} n_B r_{12}^3 \right] \ . \qquad (21)$$

In the case of a correlated medium the evaluation of the nearest-neighbor distribution is a rather involved task. For details we refer to Appendix B.

For the subsequent derivations we divide the multiquark system into free quarks and quarks in bound states. Furthermore, in calculating the interaction between unbound quarks any correlations in the distribution function are neglected. This corresponds to the independent particle picture described within the Hartree approximation (for the exchange contributions see Appendix A). The effective interaction between two free (unbound) quarks is then given by

$$V^{\text{eff}}(r_{12}) = V^{\text{conf}}(r_{12})c(r_{12})$$
$$= V^{\text{conf}}(r_{12})p_{\gamma_1\gamma_2}(r_{12})/n_B \ , \qquad (22)$$

where the probability that a string between the particles at r_1, r_2 will be realized is accounted for by the function $c(r)$. Inserting (20) or (21) into (22) one sees that the effective mean potential $V^{\text{eff}}(r_{12})$ vanishes for $r_{12} \to \infty$, although the confinement potential V^{conf} diverges. This desirable feature of the nearest-neighbor approximation introduced above does also apply in the general problem of a correlated medium, because the normalization condition (18) has to be satisfied in any case. Therefore the saturation of the confinement interaction removes the divergencies occurring, e.g., in the virial expansion with a confinement potential $V^{\text{conf}}(r_{12})$. This Hartree approximation together with the resulting saturation properties may also be applied to the quark-antiquark interaction in the case of finite temperatures $T \neq 0$ (see Ref. 13).

Notice that the Hartree approximation (uncorrelated quark distribution) reflects the quasifree motion of the quarks under frequent changes (flips) of the string interaction. This approximation is only justified in the high-density case (overlapping nucleons) but is not applicable for the low-density phase where matter is built up by nucleons and where strong correlations occur among the constituent quarks. It is an advantage of our approach that the appearance of correlations (cluster formation) in the low-density case is automatically taken into consideration, see Secs. V and VI.

For only three-quark color-singlet clusters as considered in this paper, the distribution of two quarks in a three-quark cluster cannot be calculated via $p^{(2)}_{\gamma_1\gamma_2}(r_{12})$. This is because any two quarks denoted by 2 and 3 must not be next neighbors if quark 2 is next neighbor to 1 and simultaneously if quark 3 (different color) is also next neighbor to quark 1. In this case a string separation of wrong size between the quarks 2 and 3 may occur. For independent particles (see Appendix B) the following approximate two-particle probability for the two-quark separation distribution within a composite of three quarks (color singlet) can be obtained:

$$p^{(3)}_{\gamma_1\gamma_2}(r_{12}) = \tfrac{3}{2} n_B \int_0^\infty dx \int_{-1}^1 dz\, x^2 \exp[-x^3 - (x^2+y^2-2xyz)^{3/2}], \quad y = (4\pi n_B/3)^{1/3} r_{12} \ . \qquad (23)$$

This distribution function $4\pi r_{12}^2 p^{(3)}_{\gamma_1\gamma_2}(r_{12})$ is shown in Fig. 2 together with the probability distribution function Eq. (21) of free quarks $4\pi r_{12}^2 p^{(2)}_{\gamma_1\gamma_2}(r_{12})$. It is seen that compared to the free pair distribution $p^{(2)}$ the pair distribution in three-quark systems has a maximum value shifted to larger string lengths. This is due to the fact that the minimum potential energy of a three-quark cluster is not always found from next-neighbor string configurations. The difference in the string distribution functions $p^{(2)}$ and $p^{(3)}$ leads to different mean values as

$$\langle r_{12}^2 \rangle^{(3)} = 2.0 \langle r_{12}^2 \rangle^{(2)} = 0.695 n_B^{-2/3} \ ,$$

$$\langle |r_{12}| \rangle^{(3)} = 1.4 \langle |r_{12}| \rangle^{(2)} = 0.774 n_B^{-1/3} \ , \qquad (24)$$

$$\langle |r_{12}|^{-1} \rangle^{(3)} = 0.74 \langle |r_{12}|^{-1} \rangle^{(2)} = 1.620 n_B^{1/3} \ .$$

Since free quarks move in the uncorrelated medium relatively freely, the strings may flip rather frequently from one next neighbor to another, whereas quarks which are bound into clusters are strongly correlated. We suppose that the interaction must be operative during a long time
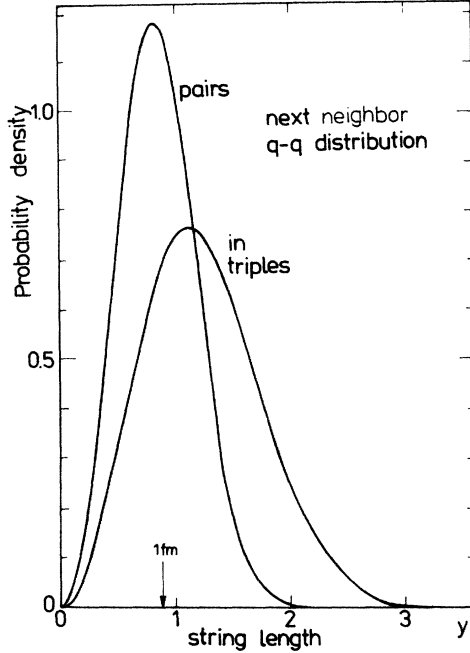
FIG. 2. Probability distribution of string lengths for uncorrelated quark distributions as a function of the reduced length $y = r_{12}(4\pi n_B/3)^{1/3}$ (scaling 1 fm for nuclear matter density ρ_0).

rate correlation effects. The approximation made here resembles the analogous treatment of a plasma when bound and scattering states are energetically well separated. In this case, scattering states behave differently from bound states and may be treated in Born approximation, whereas the bound state is treated by considering an infinite ladder sum. However, this picture is not well justified if the bound states merge into the continuum of scattering states (Mott transition).

We would like to emphasize that for color confinement the three-body correlation should also be incorporated. The decomposition of the three-body correlation into two-body correlations and the use of a modified two-body nearest-neighbor probability as given by (23) is an approximation to the three-body correlation appearing in the system consisting of unbound quarks.

interval in order that a bound state can be formed in the spirit of the infinite-ladder summation procedure. That is, we assume that the constituents of a bound state remain next neighbors for a long-time instant and that the resulting effective interaction potential associated with the rather stable bound-state string configuration is not affected by the presence of other particles.

Bearing this in mind, we take for $V^{\text{eff}}(r_{12})$ the unscreened confinement interaction $V^{\text{conf}}(r_{12})$ within a color-neutral bound-state cluster but for free quarks we shall employ the interaction $V^{\text{conf}}(r_{12})c(r_{12})$, which is screened due to the saturation by next neighbors.

In principle, the determination of $c(r_{12})$ and $V^{\text{eff}}(r_{12})$ should be performed self-consistently in order to incorpo-

V. MODEL CALCULATIONS

In order to demonstrate the applicability of the theory developed in Secs. III and IV and to discuss the consequences of the Pauli-blocking mechanism, we study a simple model case with the confinement potential

$$V^{\text{conf}}(r_{12}) = \frac{m\omega^2}{2}r_{12}^2 . \tag{25}$$

This simple quadratic confinement potential has also been employed in recent investigations within the string-flip model.[9–12] A more realistic model of confinement quark potential is considered in the next section.

One of the main advantages of the quadratic confinement potential (25) is that the three-particle Schrödinger equation can be solved exactly. The ground-state energy for the isolated nucleon is $(\hbar=c=1)$

$$E^0_{\nu_0 P} = \frac{1}{6m}P^2 + 3\sqrt{3}\,\omega + 3m , \tag{26}$$

where the internal quantum number ν_0 denotes the 1s state in the proton $(p\uparrow,p\downarrow)$ or neutron $(n\uparrow,n\downarrow)$ configuration. The corresponding wave function for the isolated three-quark bound state reads[5,11]

$$\psi^0_{\nu_0 P}(123) = \delta(P - P_R)(\sqrt{3}\,b^2/\pi)^{3/2}\exp(-b^2 p_{\xi_1}^2)\exp(-3b^2 p_{\xi_2}^2/4)P_{\text{SFC}(\nu_0)}(123) , \tag{27}$$

with $b^2 = (\sqrt{3}\,m\omega)^{-1} = \langle(r_i - R)^2\rangle = \langle r_{12}^2\rangle/3$; $P_R = p_1 + p_2 + p_3$; $p_{\xi_1} = (p_1 - p_2)/2$; $p_{\xi_2} = (p_1 + p_2 - 2p_3)$. The spin-flavor-color $[P_{\text{SFC}(\nu_0)}]$ part is antisymmetric in the color variables, but symmetric with respect to SF, and has the more explicit form[16]

$$P_{\text{SFC}(\nu_0)}(123) = \frac{1}{\sqrt{6\times 18}}(2u\uparrow u\uparrow d\downarrow + 2u\uparrow d\downarrow u\uparrow + 2d\downarrow u\uparrow u\uparrow - u\uparrow u\downarrow d\uparrow - u\uparrow d\uparrow u\downarrow - u\downarrow u\uparrow d\uparrow - u\downarrow d\uparrow u\uparrow$$

$$-d\uparrow u\uparrow u\downarrow - d\uparrow u\downarrow u\uparrow)\det|RBG| . \tag{28}$$

Making use of a perturbative treatment, the energy shift ΔE^{Pauli}, Eq (12), due to the Pauli blocking can be expressed in terms of the wave function (27). Handling carefully the SFC part, the resulting energy shift of the three-quark system due to the presence of bound states (nucleons) in the surrounding medium is

$$\Delta E_{v_0 P}^{\text{Pauli, bound}} = \frac{3\sqrt{3}}{32\sqrt{\pi}} \frac{1}{mbP} \int_{-\infty}^{\infty} dP' P' \{ [204 - 2\sqrt{3}\, b^2 (P + P')^2] e^{-(P - P')^2 b^2 / 12}$$

$$- [51 - 2\sqrt{3}\, b^2 (P + P')^2] e^{-(P - P')^2 b^2 / 3} \} f_3(E_{v_0 P'}) \ . \tag{29}$$

Here, at $T = 0$ the P' integral is restricted to the region $P' \le P_F^h$, where P_F^h denotes the Fermi momentum of the hadrons corresponding to the hadronic density n_h:

$$P_F^h = (3\pi^2 n_h / 2)^{1/3} \ . \tag{30}$$

Expanding the integrand of Eq. (29) with respect to P, P' one has, to lowest order,

$$\Delta E_{v_0 P}^{\text{Pauli, bound}} \approx \frac{17\sqrt{3}\, b^3}{32\sqrt{\pi}\, m} [\tfrac{1}{5} (P_F^h)^5 + \tfrac{1}{3} (P_F^h)^3 P^2] \ . \tag{31}$$

For $T = 0$, and according to Eqs. (9) and (13) the energy shift $\Delta E_{v_0 P_F^h}^{\text{Pauli}}$ at the Fermi momentum is related to the quark chemical potential μ through

$$E_{v_0 P_F^h}^0 + \Delta E_{v_0 P_F^h}^{\text{Pauli, bound}} = 3\mu \ . \tag{32}$$

Let us briefly discuss the case of completely hadronized quark matter, $n_B = n_h$. With (26), (31), and (32) we have the relation

$$\mu(n_B, T = 0) = \sqrt{3}\,\omega + m + \frac{1}{18m} \left[\frac{3\pi^2}{2} n_B \right]^{2/3}$$

$$+ \frac{17\sqrt{3}}{60\sqrt{\pi}} \frac{b^3}{m} \left[\frac{3\pi^2}{2} n_B \right]^{5/3} , \tag{33}$$

which can be interpreted as the equation of state for the case where a bound-state quark cluster (nucleon) is surrounded by only bound-state quark clusters (nucleons). In other words, we have deduced an equation of state of hadronic matter in a simple approximation, where in addition to the ideal Fermi-gas treatment of the nucleons the Pauli-blocking effects due to the quark structure are taken into account.

We have evaluated the shift $\Delta \mu = \mu(n_B, T = 0)$ $-\mu(n_B = 0, T = 0)$, see Fig. 3. The parameters $m = 350$ MeV, $b = 0.59$ fm entering (33) have been taken from Oka and Horowitz,[11] who were able to describe the low-lying nucleon energy spectrum and the $^1S_0$ nucleon-nucleon scattering phases at high energies. Especially, the fairly good reproduction of the high-energy nucleon-nucleon scattering data within their string-flip model stresses the importance of retaining the antisymmetrization among the quark constituents in order to generate the repulsive part of the nucleon-nucleon interaction. This effect is well known from the interaction between atoms or molecules, where, because of the consideration of the Pauli principle with respect to the electrons, effective potentials become apparent which are strongly repulsive. Also in our approach, which for the two-nucleon problem is very similar to that of Oka and Horowitz,[11] it is expected that the scattering phases are reproduced for high energies. We are, however, not interested in these two-nucleon characteristics but rather in the bulk properties of nuclear

matter described within an underlying quark picture. One interesting quantity to be studied in the many-body system is the chemical potential, because according to the well-known Beth-Uhlenbeck formula the scattering phase shifts determine the thermodynamic properties of the system. Thus, instead of comparing with experimental scattering phases we are attempting to compare with results inferred from a theoretical description of known nuclear matter properties at zero temperature.

Here we considered only the antisymmetrization among the quarks. However, it was pointed out by Oka and Yazaki[17] (see also Ref. 4) that the spin-spin interaction between the quarks plays also an important role in calculating the effective repulsion. The spin-spin contribution (V_{ij}^{short}) is considered in the next section.

Let us first consider in Fig. 3 the shift of the chemical potential $\Delta \mu$ which gives us information on the relevance of the Pauli-blocking effect. An essential feature of $\Delta \mu$ is its steep increase with the baryon-number density n_B. This is solely due to the consideration of the Pauli principle with respect to the quarks. The blocking of phase space by the surrounding hadrons quenches the considered bound state implying that the bound state itself becomes energetically unfavorable. Notice that this effect is not linear in n_B, but proportional to $n_B^{5/3}$, which arises from the consideration of the Pauli principle with respect to the
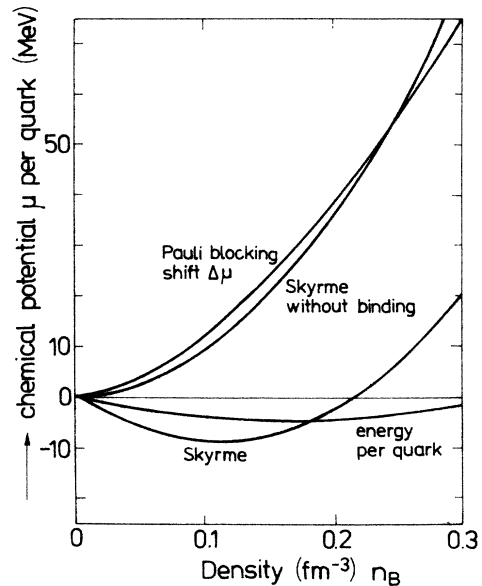

FIG. 3. Equation of state $\Delta \mu$ from Eq. (33), $\Delta \mu = \mu(n_B, T = 0) - \mu(n_B = 0, T = 0)$ compared with the Skyrme expression (34) and Skyrme without binding [$a = 0$ in Eq. (34)]. Furthermore, the free energy per quark (35) is presented which coincides at $T = 0$ with the internal energy per quark.

hadrons, i.e., the consequence of the fact that not only the self-energy diagram but also the hadronic exchange diagram has been taken into account, cf. (A6).

It is now interesting to see how these results for $\Delta\mu$ compare with an empirical fit to the chemical potential of ordinary nuclear matter. We take the Skyrme-type parametrization of Vautherin and Brink[18] widely used to calculate nuclear matter (NM) properties:

$$3\Delta\mu_{\text{NM}}^{\text{Skyrme}} = \frac{1}{2M} \left[\frac{3\pi^2}{2} n_B \right]^{2/3} + an_B + bn_B^{5/3} + cn_B^2 \quad (34)$$

with the choice of parameters $a = -792.97$ MeV fm^3, $b = 125.225$ MeV fm^5, $c = 2711.9$ MeV fm^6, M is the nucleon mass. The free energy per quark $f(n_B, T=0) = f(n_B=0, T=0) + \Delta f$ of nuclear matter at zero temperature is obtained according to (15):

$$3\Delta f_{\text{NM}} = \frac{3}{10M} \left[\frac{3\pi^2}{2} n_B \right]^{2/3} + \frac{1}{2}an_B + \frac{3}{8}bn_B^{5/3} + \frac{1}{3}cn_B^2 \quad (35)$$

and coincides with the internal energy per quark of nuclear matter at $T=0$. The parameter choice of Vautherin and Brink[18] fits the empirical nuclear matter data; i.e., the minimum of the free energy is found at $\rho_0 = 0.17$ fm^{-3} with the binding energy per nucleon $E_B = -16$ MeV (see Fig. 3).

The binding properties of nuclear matter are accounted for by the linear term in the density in Eq. (34). Of course, within our simple approach we do not reproduce a binding part of the hadron-hadron interaction. This may be realized by the exchange of virtual pions, i.e., by virtual quark-antiquark excitations neglected in our approach. Disregarding the binding property of the Skyrme parametrization, i.e., considering $\Delta\mu_{\text{NM}}^*$ by setting $a = 0$ in Eq. (34), then the shifts $\Delta\mu$ and $\Delta\mu_{\text{NM}}^*$ agree surprisingly well as can be seen from inspection of Fig. 3. We are aware of taking this agreement too seriously but it may indicate to what extent a nuclear matter equation of state based on a quark picture may reproduce some of the expected "empirical" properties of nuclear matter.

Notice that the expression (29) permits us also to study the temperature dependence of the Pauli-blocking or phase-space occupation due to the quarks forming composites and the free quarks as well. In a recent paper[19] the effective mass has been calculated for a nucleon moving in a finite-temperature medium. It turned out that for $T=0$ the results coincide surprisingly well with those obtained from ordinary Hartree-Fock calculations. The solution of the effective wave equation corresponding to the Bethe-Goldstone equation (A3) leads to temperature- and density-dependent nucleonic wave functions permitting us to estimate the increase of the average nucleon radius due to the presence of matter (EMC effect).

In perturbation treatment and by using the wave function (27), the shift of the nucleon energy due to free quarks is given by

$$\Delta E_{v_0 P}^{\text{Pauli, free}} = \frac{9\sqrt{3}}{4\sqrt{2\pi}} \frac{1}{mbP} \int_{-\infty}^{\infty} dp\, p[7 - 3b^2(P/3-p)^2]\exp\left[-\frac{3}{2}b^2 \left[\frac{P}{3} - p \right]^2 \right] f(E_p) \quad (36)$$

and illustrates that free quarks are very effective in blocking out bound states. This effect results in a large shift especially for $P=0$. With increasing density the states near $P=0$ are shifted so far that the formation of bound-state clusters with $P\neq0$ in free quark matter becomes more favorable.

The free-particle energy shift Δ^H in the Hartree approximation is evaluated after replacing the confinement potential $V^{\text{conf}}(r)$ by an effective density and temperature-dependent potential $V^{\text{eff}}(r)$ as introduced in Sec. III, and therefore the determination of the Hartree shift should be done with care. The basic idea behind the Hartree approximation is that the pair-distribution function is assumed to be uncorrelated, $\rho_{a_1 a_2}(r_{12}) = n_B^2/16$. The potential energy per quark E_{pot} for the free-quark system follows from the string energies, and with (20) and (21) we have in a system of free quarks

$$E_{\text{pot}} = \int d^3r\, V^{\text{eff}}(r) . \quad (37)$$

Making use of relation (16) and under consideration of (24) one finds

$$\Delta^H = \frac{1}{3} \frac{m\omega^2}{2} \langle r_{12}^2 \rangle^{(3)} . \quad (38)$$

In the case that all bound states are blocked out (quark matter) the equation of state is immediately evaluated. The associated chemical potential takes the form

$$\mu(n_B, T=0) = \frac{1}{2m} \left[\frac{3\pi^2}{2} n_B \right]^{2/3}$$

$$+ 0.0386\frac{1}{mb^4}n_B^{-2/3} + m . \quad (39)$$

The most striking effect in the free quark system of low density (neglecting all correlations between the quarks) is the increase of energy and chemical potential when decreasing the density. This is in contrast with the nuclear matter properties at low density and is the consequence of the confinement phenomenon. In this low-density case, the confinement potential is saturated at large mean distances.

The general equation of state $\mu(n_B, T=0)$ is obtained for a homogeneous system from Eqs. (9) and (13) where bound states (hadrons) as well as free quarks may occur. The result for the quadratic confinement potential is shown in Fig. 4(a). At low density, the chemical potential μ of the hadronic matter is lower than the free-quark
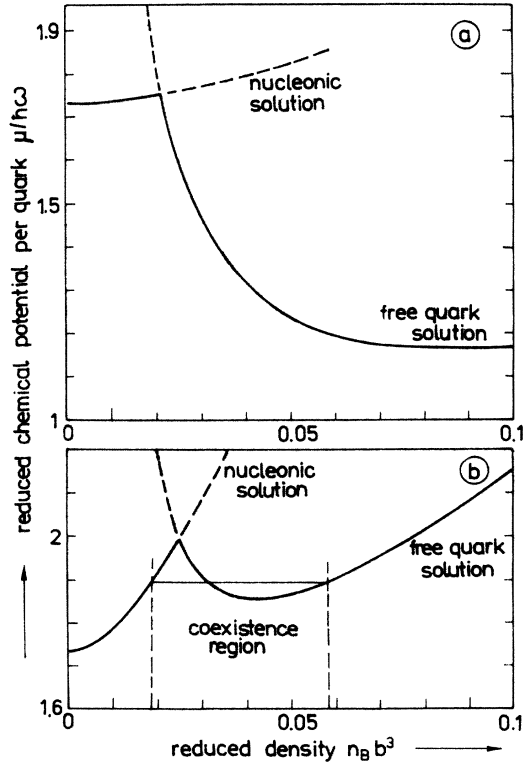
FIG. 4. Equation of state $\mu(n_B, T = 0)$ for the quadratic confinement Eq. (25). (a) Fourfold spin-flavor degeneration, (b) no spin-flavor degeneration.

Hartree energy, so that the free-quark states cannot be occupied. Thus, we have a system of hadrons in the environment of hadrons. If the baryon-number density is larger than the value $n_B = 0.021b^{-3}$, the free-quark Hartree shift becomes smaller than the bound quark chemical potential so that the free-quark states can be filled. Because of free quarks, the bound-state energy is lifted up so far that the system may flip suddenly to the free-quark solution. No solution of (13) has been found which corresponds to a partially hadronized quark matter. Going from high to low density, the free-quark solution for $\mu(n_B, T = 0)$ indicates that the formation of bound states embedded in surrounding free-quark medium is allowed for densities below $n_B = 0.015b^{-3}$.

An important feature of the equation of state is that it gives information on the thermodynamic stability of matter. If the condition of stability $\partial\mu/\partial n_B \mid_{T=0} \geq 0$ is violated, the homogeneous state becomes unstable with respect to phase separation. The region of the two-phase coexistence is obtained from a Maxwell construction in the representation $\mu = \mu(n_B, T)$ or, more generally, from the double tangent construction for the free energy.

For the simplified quadratic confinement potential model and degeneration 4 with respect to spin and flavor (SF), no stable hadronic matter is obtained, see Fig. 4(a), because the absolute minimum of the free energy occurs in the free-quark phase at too-large densities of about $n_B = 0.24b^{-3}$. In the next section we show that for a more realistic model of confinement quark potential the

condition that the hadronic phase is stable is satisfied. In order to simulate the case of a stable hadronic phase below a critical density n_B^c, a model calculation for the quadratic confinement potential having no degeneration with respect to spin and flavor is shown in Fig. 4(b). In spite of the fact that the results in Fig. 4(b) are not realistic because of neglect of spin-flavor degeneration, they illustrate clearly that the stability of hadronic matter is very sensitive to the spin and flavor degrees of freedom.

The model calculations of this section have shown that some important features of the empirical nuclear matter properties can be well reproduced on the basis of the underlying quark substructure. However, the more reliable calculation of the transition region from stable hadronic matter can only be achieved with a better potential model to be considered in the next section.

VI. MORE REALISTIC MODEL CALCULATIONS

Applying the quark potential model to real matter, the form of the potential must be better specified and parametrized. For instance, one may use a potential similar to those treated in the very successful approaches to six-quark systems:[6,11]

$$V = \sum_{i<j} (\lambda_i \lambda_j)(V_{ij}^{\text{conf}} + V_{ij}^{\text{short}}) ,$$

$$V_{ij}^{\text{conf}} = -\tfrac{3}{8}(ar_{ij}^2 + C) ,$$

$$V_{ij}^{\text{short}} = \tfrac{1}{4}\alpha_s \frac{1}{r_{ij}} - \frac{1}{16m^2}\Delta V_{ij}(1 + \tfrac{8}{3}\mathbf{s}_i\mathbf{s}_j) + U(r_{ij}) , \quad (40)$$

$$V_{ij} = \tfrac{1}{4}\alpha_s \frac{1}{r_{ij}} + \epsilon V_{ij}^{\text{conf}} .$$

In $U(r_{ij})$ further short-range modifications of the quark-quark interaction (e.g., tensor forces) are collected which are dropped here. With $C = 0$, $\epsilon = 0$, this choice of the quark potential coincides with that of Oka and Horowitz.[11] Taking their parameter values $\alpha_s = 1.77$, $m = 350$ MeV, $a = \tfrac{1}{6}$ 230 MeV/fm^2 one reproduces not only the baryon data but also the NN scattering phase shifts at high energies.

For the sake of continuity we will utilize this set of parameter values and take $C = 54.48$ MeV to adjust the nucleon mass (see Appendix C). For the variational parameter b in the Gaussian-type wave function (27) the optimal value $b = 0.59$ fm^{-1} is obtained by minimizing the nucleon binding energy.

Within this more realistic quark potential model, the free energy per quark f at zero temperature as function of the baryon density n_B is shown in Fig. 5. In the hadronic phase, the energy shift $\Delta E_{v_0P}^{\text{Pauli}}$ due to the Pauli-blocking mechanism is calculated from the wave function of the three-quark bound state and the quark mass, cf. Eq. (12). Because the quark-model potential does not appear explicitly, one may use the results obtained in Sec. V. It was found that the empirical nuclear matter result[18] for the free energy f^h per quark (in MeV, n_B in fm^{-3})

$$f^h(n_B, T = 0) = 313 + 24.75n_B^{2/3} - 132.16n_B$$
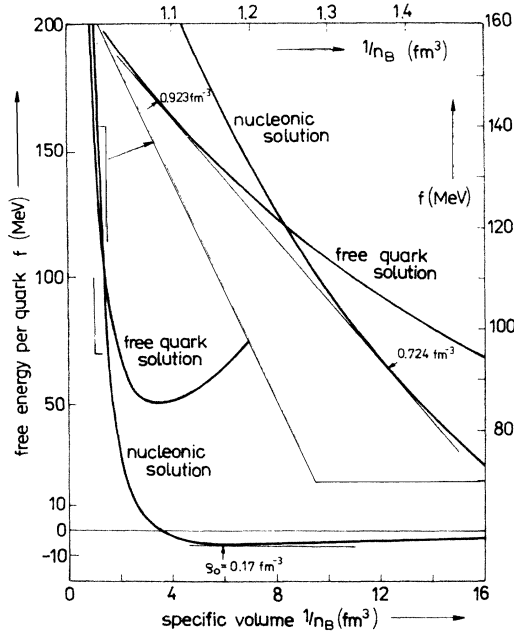$$+ 301.32n_B^2 + 15.65n_B^{5/3} \quad (41)$$

FIG. 5. Equation of state $f(n_B^{-1}, T=0)$ for a realistic quark potential model, Eq. (40), according to Eqs. (41) and (42). The empirical version, Eq. (41), of the equation of state in the hadronic phase includes a binding part, cf. Fig. 3. Double tangent construction gives two phase transitions: from $n_B=0$ to nuclear matter density ρ_0 and the quark/nuclear matter phase transition (see the insertion).

can also be reproduced in a good approximation within our approach if one would add to (29) an empirical binding-force contribution [see also discussion below Eq. (35)]. A quite similar situation exists in calculating the N-N interaction.[11,17] There the attraction between nucleons may be introduced as the effect of a meson cloud which has not been considered here.

According to (37) and using the quark potential (40) the free energy per quark in the free-quark phase is given by the expression (cf. Appendix C)

$$f^{\text{free}}(n_B, T=0) = 69.72 \times 10^3 \frac{1}{m} n_B^{2/3} + 0.695 a n_B^{-2/3}$$

$$- 212.03 \alpha_s n_B^{1/3}$$

$$+ 15.85 \times 10^6 \alpha_s \frac{1}{m^2} n_B$$

$$+ 57.82 \times 10^3 \frac{a}{m^2} \epsilon + C + m \ . \quad (42)$$

Since an averaging over the spin states has been performed, the spin part of (40) does not contribute to the free energy f^{free}.

The free energies per quark for the hadronic phase as well as the free-quark phase are given in Fig. 5 as a function of n_B^{-1}. Possible phase separation regions due to the appearance of a first-order phase transition are obtained from a double tangent construction. As shown in Fig. 5, two distinct phase transitions are obtained from our

model calculation at zero temperature. The first one is the liquid-gas-like phase transition in nuclear matter.[20] At zero temperature the associated region of instability reaches from $n_B=0$ to nuclear matter density $n_B=\rho_0$ $=0.17$ fm^{-3}. This phase transition exists for temperatures lower than a critical one of about 15—20 MeV. The second phase transition is associated with a transition from nuclear matter to quark matter and occurs at density values between $n_B^{\text{I}}=4.26\rho_0$ and $n_B^{\text{II}}=5.43\rho_0$. This can be seen from the double tangent construction displayed also in Fig. 5. The density values for the transition region are in reasonable good agreement with the findings of other approaches.[21]

The results of the calculations shown in Fig. 5 illustrate that within the more sophisticated confinement potential model (40) which reproduces the properties of nucleons and two-nucleon characteristics, also a phase transition to quark matter is obtained. The nature of this new phase is characterized by the absence of bound states (nucleons) which are dissolved by virtue of the Pauli-blocking mechanism. A similar effect is known in nuclear matter as well as in plasma and solid-state physics (Debye screening) where it is called the Mott effect. A Mott mechanism due to color screening was recently studied by Satz.[22] This mechanism is not considered in this paper in which the action of the Pauli principle has been taken into account.

There are further potentials discussed in the literature[23] such as, e.g., a linear confinement potential

$$V_{ij}^{\text{conf}} = -\frac{3}{8}(\lambda r_{ij} + C) \ , \quad (43)$$

and the incorporation of the confinement potential into the Darwin term and the spin-spin term.[5] Different parameter values were considered by adjusting the low-lying baryon masses. The dependence of the equation of state on various parameter-value choices is discussed in Appendix C, and we show that the gross behavior of the equation of state and the occurrence of a phase transition is not influenced remarkably by different forms of the quark-quark potential.

Before the nuclear-to-quark-matter phase transition found in our model can be brought in close connection with the expected phase transition in real matter one has to investigate further mainly two problems: (i) to what extent the approximation scheme in deriving the equation of state within the potential model is correct and (ii) how realistic the use of the potential model for overlapping nucleons is. With respect to (i), the influence of the quark potential parameters, the effect of virtual quark-antiquark excitations, the extension of possible string configurations including three-body string and non-next-nearest interactions, and the inclusion of further diagrams in evaluating the Green's functions seems to be of vital interest, and should be the subject of further work. Let us remember that Horowitz et al.[9] solved the Schrödinger equation for a quark potential model using numerical methods. However, they could not observe a phase transition because a one-dimensional problem was solved. Furthermore, they considered a system with a finite number of quarks. It is worthwhile to note that the qualitative behavior of their

results with respect to the pair correlation function coincides with our findings that the bound-quark states are dissolved with increasing density. In a recent paper[24] by Horowitz the calculations of Ref. 9 has been extended to the three-dimensional case. He also found that the quark correlation function is significantly modified if a nucleon is embedded in nuclear matter.

With respect to (ii) we should in general expect that the quark potential model may only be applied for density values of quarks which do not exceed the density within a nucleon. As is well known, at high densities another form of the equation of state of matter is obtained from perturbative quantum chromodynamics (see Ref. 23). The region of applicability of the simplified quark potential model can only be established from a more fundamental derivation of this model within QCD. Finally it should also be remembered that one has to pass from the equilibrium thermodynamics to a nonequilibrium theory if one is looking for the effects of the equation of state of quark/nuclear matter in high-energy collision processes.

VII. CONCLUDING REMARKS

Our main task was to try a unique description of quark and nuclear matter within a simple quark potential model. Before applying the standard formalism of the many-body theory, we had to realize the saturation property of the string interaction so that the particularities due to the confinement interaction can be removed. The most important in-medium effect which has to be incorporated is the action of the Pauli principle between the quark constituents of the nucleons. The Pauli-blocking gives rise to a shift of the nucleonic quasiparticle energies in dependence on baryon-number density, temperature and nucleon momentum. It is interesting to remark that such a model calculation reflects quite well the short-range behavior of the empirical Skyrme interaction in nuclear matter and can be immediately extended to finite-temperature values. A consequence of the Pauli-blocking is that the bound-state quark clusters (hadrons) become energetically unfavorable at high densities, so that a transition to a free-quark phase takes place. The quark potential model permits us to apply the methods of quantum statistics, but in general its range of applicability has to be determined through QCD.

ACKNOWLEDGMENTS

APPENDIX A: APPROXIMATE EVALUATION OF THE GREEN'S FUNCTIONS

Let us use a diagrammatic representation, so that the Dyson equation reads

$$G_1(1,z) = \quad \quad \quad \quad \quad \quad \quad . \tag{A1}$$

The self-energy $\Sigma(1,z)$ is represented by a cluster decomposition which gives in the ladder-Hartree-Fock approximation, cf. Ref. 15,

$$\tag{A2}$$

where t_n^b denotes the bound-state part of the n particle t matrix defined according to

$$\tag{A3}$$

with

$$V_{1,n}(1,\ldots,n,1',\ldots,n') = \sum_{i=2}^{n} V(1i,1'i') \prod_{j \neq 1,i} \delta_{jj'}$$

(which has to be antisymmetrized),

$$K_n = \sum_{i<j} V_{ij}(ij,i'j') \prod_{k \neq i,j} \delta_{kk'} + \Delta K_n \; ;$$

$$G_n^0(1,\ldots,n,1',\ldots,n'_1\Omega_n)$$

$$= \sum_{z_1 \cdots z_{n-1}} \frac{1}{z_1 - E(1)} \cdots \frac{1}{z_{n-1} - E(n-1)}$$

$$\times \frac{1}{\Omega_n - z_1 - \cdots - z_{n-1} - E(n)} \; . \tag{A4}$$

In (A2), the Fock term has not to be considered because interaction between quarks of equal color does not occur in our model. Furthermore, two-body bound states (t_2^b) are not considered because antiquark and meson formation is not treated within this paper. For the more general case see Ref. 13. Therefore, only the Hartree term and the three-particle cluster (nucleon) contribution (t_3^b) survive.

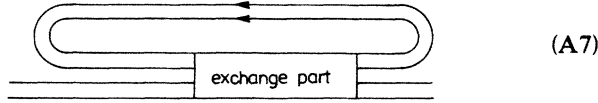Now, let us consider t_3^b more in detail. For G_3^0 we find

$$G_3^0(123,1'2'3',\Omega_3) = \frac{[1-f_{\alpha_1}(1)][1-f_{\alpha_2}(2)][1-f_{\alpha_3}(3)] - f_{\alpha_1}(1)f_{\alpha_2}(2)f_{\alpha_3}(3)}{\Omega_3 - E(1) - E(2) - E(3)} \delta_{11'}\delta_{22'}\delta_{33'} \; . \tag{A5}$$

In calculating the medium effects we have to select out the relevant diagrams contributing to ΔK_n. We choose

$$\quad (A6)$$

(crosses denote amputation at equal time), and we give the following arguments: Generally, a t matrix has a structure as depicted in (A7)

$$\quad (A7)$$

It consists of a forward-directed part with interactions, an exchange part, and a backward-directed one determining the order of fugacity. We are looking for terms which are proportional to the free-particle density (one backward line) and those proportional to the cluster density [one clustered backward line, see (A8)]. Furthermore, we consider interactions only within color neutral composites, not between them. In the spirit of a Born expansion the following types of diagrams should be regarded:

$$\quad (A8)$$

The first one (i) is always contained in G_3^0 and has to be dropped. Diagrams (ii) and (iii) are the relevant ones and can be transformed in those given in (A6). A further exchange of lines in (A8) gives no topologically new terms and must not be considered.

This selection of relevant diagrams is equivalent to the introduction of a chemical picture, where bound states are treated on the same footing as free particles. For the evaluation of the diagrams, the solution of the t-matrix equation or the corresponding homogeneous wave equation (effective Schrödinger equation for a three-particle system with an effective potential containing the influence of the surrounding medium) and the use of perturbation theory we refer to standard textbooks (see also Ref. 15). We remark that within a more sophisticated approximation the three-particle binding energy $E_{\nu P}^0$ in Eq. (12) will be replaced by the kinetic energy of the bound state.

The approximations for the two-particle Green's function (8) are performed in the same way as for (A2):

$$\quad (A9)$$

which is solved by standard methods. Notice that $\longmapsto$ is immediately connected with the total single-particle densi-

ty according to (7). In (A8) we remark that no self-energy is considered, because the interaction is restricted to be operative only within the three-body clusters.

APPENDIX B: NEXT-NEIGHBOR DISTRIBUTION FUNCTION

The determination of the distribution of string lengths for a given configuration of quark positions is a rather involved problem when dealing with correlated quark matter. The quantity to be optimized is the potential energy which is proportional to $\langle |r_{12}|^2 \rangle$ according to the choice (25) of the potential. The rigorous solution of this problem can be given here only for the case of two-particle clusters in uncorrelated quark matter. For this, the solution (20) of (19) can immediately be used for the string distribution, because quarks of different color are considered as statistically independent. An exchange contribution leading to a Fock term in the mean potential energy will not occur because the interaction $V^{conf}(r_{12})$ vanishes if both colors coincide.

Another solution of Eq. (19) denoted by $c^{Fermi}(r)$ is obtained from an expression for $\rho_2(r-r')$ taking into account the formation of a Fermi hole. For a system of identical fermions having no internal degrees of freedom, the pair distribution function $\rho_2(r-r')$ at $T=0$ behaves near $r=r'$ like $(r-r')^2$ due to the Pauli principle. From (19) it follows that, for small values of r,

$$c^{Fermi}(r) = \exp(-\alpha r^5) . \quad (B1)$$

Adopting this functional dependence for the entire space, the parameter α can be determined by the normalization condition (18) and takes the value $\alpha = 3.743 n_B^{5/3}$.

In this paper we took for the model calculations two spin directions and two flavors. Since the Pauli principle acts only between quarks of identical spin and flavor, the formation of a Fermi hole is strongly reduced and is finally neglected in the subsequent calculation.

Let us now consider the probability distribution $p_{\gamma_1\gamma_2}^{(3)}(r_{12})$ for the two-quark separation within a three-quark color-neutral singlet. The problem of the determination of the string length distribution function $p_{\gamma_1\gamma_2}^{(3)}(r_{12})$ for a system of uncorrelated quarks with three quark cluster configuration of minimum confinement energy also cannot be solved in a rigorous manner. Let us consider the probability that three next-neighbored quarks with respect to a given central point ($r=0$) are located at r_1, r_2, r_3. The two next-neighbored quarks are then distributed with the density

$$\rho_{\gamma_1\gamma_2}^{n,n}(r_1,r_2) = n_B^2 \exp\left[-\frac{4\pi}{3} n_B(|r_1|^3 + |r_2|^3)\right] . \quad (B2)$$

The probability distribution of the distance $r_{12} = r_1 - r_2$ between these nearest neighbors is obtained from

$$4\pi r_{12}^2 p_{\gamma_1\gamma_2}^{(3)}(r_{12}) = \int d^3r_1 \int d^3r_2 n_B^2 \exp\left[-\frac{4\pi}{3} n_B(|r_1|^3 + |r_2|^3)\right] \delta(r_{12} - [r_1^2 + r_2^2 - 2r_1 r_2 \cos(e_1,e_2)]^{1/2}) \quad (B3)$$

which leads to Eq. (23) after performing some integrations.

Notice that the distribution (B2) corresponds more naturally to the three-body string configuration, cf. Fig. 1(b), which may be energetically favored, and especially a permanent string-flip process in the free-quark matter state may be represented more adequately by this three-body string configuration.

APPENDIX C: NUCLEAR MATTER/QUARK PHASE TRANSITION FOR DIFFERENT QUARK INTERACTION POTENTIALS

At the end of Sec. V it was shown that the occurrence of a phase transition from the free-quark phase to a stable hadronized phase depends sensitively on the form of the quark interaction potential as well as number of the spin and flavor degrees of freedom [cf. Figs. 4(a) and 4(b)]. It is of interest to investigate the occurrence of this phase transition in dependence of the form and parametrization of the considered quark interaction potential. We consider four types of interactions frequently used in the literature.

(A) quadratic two-body string interaction

$$V_{(A)} = \sum_{i<j}^{3} \left[ar_{ij}^2 + C - \frac{2}{3}\alpha_s \frac{\hbar c}{r_{ij}} + \frac{\hbar^2}{4m^2c^2} \Delta V_{(2)}^{\epsilon}(r_{ij})[1+\frac{8}{3}(s_i s_j)] \right] , \tag{C1}$$

(B) linear two-body string interaction

$$V_{(B)} = \sum_{i<j}^{3} \left[\lambda r_{ij} + C - \frac{2}{3}\alpha_s \frac{\hbar c}{r_{ij}} + \frac{\hbar^2}{4m^2c^2} \Delta V_{(1)}^{\epsilon}(r_{ij})[1+\frac{8}{3}(s_i s_j)] \right] , \tag{C2}$$

(C) quadratic three-body string interaction

$$V_{(C)} = \sum_{i=1}^{3} \left[ar_i^2 + C - \frac{2}{3}\alpha_s \frac{\hbar c}{r_i} + \frac{\hbar^2}{4m^2c^2} \Delta v_{(2)}^{\epsilon}(r_i)[1+\frac{8}{3}(s_i s_j)] \right] , \tag{C3}$$

(D) linear three-body string interaction

$$V_{(D)} = \sum_{i=1}^{3} \left[\lambda r_i + C - \frac{2}{3}\alpha_s \frac{\hbar c}{r_i} + \frac{\hbar^2}{4m^2c^2} \Delta V_{(1)}^{\epsilon}(r_i)[1+\frac{8}{3}(s_i s_j)] \right] , \tag{C4}$$

with $\mathbf{r}_{ij} = \mathbf{x}_i \mathbf{x}_j; \mathbf{r}_i = \mathbf{x}_i - \mathbf{R}$, $\mathbf{R}$ being the center-of-mass coordinate

$$\Delta V_{(2)}^{\epsilon}(r) = \frac{2}{3}\alpha_s \hbar c 4\pi \delta^3(r) + 6\epsilon\alpha ,$$

$$\Delta V_{(1)}^{\epsilon}(r) = \frac{2}{3}\alpha_2 \hbar c 4\pi \delta^3(r) + 2\epsilon\lambda \frac{1}{r} . \tag{C5}$$

The three-quark ground state is determined via a variational calculation using Gaussian-type trial functions with the range parameter $b^2 = \hbar/\sqrt{3}m \, \omega$ in (27). The ground-state energy is evaluated with

$$E_{v_0,P=0}^0 = \frac{3}{2}\frac{\hbar^2}{m}b^{-2} + \langle V \rangle ,$$

$$\langle r_{ij}^2 \rangle = 3b^2, \quad \langle r_{ij} \rangle = \frac{2\sqrt{2}}{\sqrt{\pi}}b ,$$

$$\left\langle \frac{1}{r_{ij}} \right\rangle = \sqrt{2/\pi}\frac{1}{b}, \quad \langle \delta^3(r_{ij}) \rangle = \frac{1}{(2\pi)^{3/2}}\frac{1}{b^3} ; \tag{C6}$$

$$\langle r_i^2 \rangle = b^2, \quad \langle r_i \rangle = \frac{2\sqrt{2}}{\sqrt{3\pi}}b ,$$

$$\left\langle \frac{1}{r_i} \right\rangle = \sqrt{6/\pi}\frac{1}{b}, \quad \langle \delta^3(r_i) \rangle = (3/2\pi)^{3/2}\frac{1}{b^3} ; \tag{C7}$$

$\sum_{i<j}^{3}(s_i s_j) = -\frac{3}{4}$ in the nucleon state (N), $= \frac{3}{4}$ in the Δ state.

The parameter b is determined by the minimum of the energy (C6). With this approximate Gaussian-type wave

function and the corresponding energy eigenvalue, the Pauli-blocking energy shift of the nucleon is evaluated according to (31). For the free energy per quark f^{had} in the hadron phase we have [nuclear binding is taken into account phenomenologically by adding a term linear with respect to n_B as in the Skyrme expression (35)]

$$f^{\text{had}}(n_B, T=0) = 313 \text{ MeV} + \frac{1}{10}\frac{\hbar^2}{M}\left[\frac{3\pi^2}{2}n_B\right]^{2/3}$$

$$- \frac{1}{6}792.97 \text{ MeV fm}^3 n_B$$

$$+ \frac{17\sqrt{3}\hbar^2}{160\sqrt{\pi}m}b^3\left[\frac{3\pi^2}{2}n_B\right]^{5/3} . \tag{C8}$$

We take the nucleon mass $Mc^2 = 939$ MeV. In particular, the nuclear matter binding energy E_b is determined by $E_b = 3f^{\text{had}}(\rho_0, T=0)$ and should be compared with the empirical value -16 MeV. For the construction of the two-phase coexistence region and the corresponding boundary densities n^I, n^{II} we take the empirical free energy per quark (35) for the hadron phase, $f^{\text{had}} = 313$ MeV $+ \Delta f$, and the expression [cf. (42)]

$$f^{\text{free}}(n_B, T=0) = mc^2 + C + \frac{3}{10}\frac{\hbar^2}{m}\left[\frac{3\pi^2}{2}n_B\right]^{2/3}$$

$$+ \langle V^{\text{eff}}(r) \rangle n_B \tag{C9}$$

TABLE I. The border densities n_B^I and n_B^{II} of the hadron-to-quark-matter phase transition for different potential models (C1)–(C4) and different parameter values $\epsilon, \alpha_s, m, a, \lambda, C$. The parameter C fits the nucleon mass $Mc^2 = 939$ MeV. The range of the other parameter values was restricted so that reasonable values for the N-Δ mass difference $E_{N\Delta}$ and the nuclear matter binding energy E_b result.

Potential type	ϵ	α_s	m (MeV)	a $\left[\dfrac{\text{MeV}}{\text{fm}^2}\right]$	λ $\left[\dfrac{\text{MeV}}{\text{fm}}\right]$	C (MeV)	b (fm)	$E_{N\Delta}$ (MeV)	E_b (MeV)	n_B^I (fm^{-3})	n_B^{II} (fm^{-3})
A	0	1.77	350	38.3		54.6	0.585	290.5	-12.5	0.724	0.923
A	0	1.77	400	34		36.8	0.539	284.4	-22.6	0.562	0.781
A	1	0.5	350	150		-245.4	0.60	283.7	-10.0	0.595	1.020
A	1	1	350	70		-114.9	0.615	273.4	-7.3	0.555	0.752
A	1	1	400	90		-161.5	0.55	281.3	-21.2	0.445	0.730
B	0	0.52	270		800	-787.6	0.47	276.6	-22.9	0.40	0.926
B	0	1	300		400	-382.0	0.528	303.8	-17.0	0.549	0.781
B	1	0.52	350		250	-362.7	0.610	281.1	-8.2	0.474	0.690
C	0	0.5	440	270		-215.1	0.575	284.2	-20.3	0.442	0.971
D	0	0.5	400		320	-272.1	0.612	285.2	-12.4	0.465	0.910

for the free-quark phase. The effective potential is evaluated with the next-neighbor q-q distribution in triplets when using the potentials A,B. In the case of the potentials C,D the next neighbors with respect to the center of mass R are of relevance. The corresponding mean values are collected in Eq. (24). In the case D, e.g., we have

$$\langle V^{\text{eff}}(r) \rangle^{(2)} n_B = 0.554 \lambda n_B^{-1/3} - \tfrac{2}{3} 2.183 \hbar c \alpha_s n_B^{1/3}$$

$$+ \tfrac{2}{3} \pi \hbar^3 c^3 \frac{\alpha_s}{m} n_B + 2.183 \frac{\hbar^2}{2m} \epsilon \lambda n_B^{1/3} .$$

$$(C10)$$

The case A is given by Eq. (42).

The parameter C was adjusted to the nucleon mass M using (C6). The other parameters $\alpha_s, a, \lambda, m, \epsilon = 0, 1$ were chosen in such a manner that reasonable values for the mass difference $E_{\Delta N} = E_\Delta - E_N$ as well as for the nuclear matter binding energy E_b will be reproduced.

Results for different types of potentials $(A-D)$ for the quark interaction and for different parametrization as well are given in Table I. It is remarkable that there is no large spreading in the the the values of n_B^I and n_B^{II}, respectively, determining the borders of the phase transition at $T = 0$. Typical values are $n_B^I = 0.5$–0.6 fm^{-3} and $n_B^{II} = 0.8$–0.9 fm^{-3}. We stress also the possibility to use not only the mass spectra of the nucleons but also the nuclear matter properties (binding energy) and the stability of the hadronic phase if the quark interaction potential is determined.

[1]O. W. Greenberg, Phys. Rev. Lett. 13, 598 (1964).

[2]A. De Rújula, H. Georgi, and S. L. Glashow, Phys. Rev. D 12, 147 (1975).

[3]N. Isgur and G. Karl, Phys. Rev. D 18, 4187 (1978); 19, 2653 (1979); J. Dias de Deus and A. B. Henriques, Z. Phys. C 7, 157 (1981); A. B. Henriques and N. Isgur, Phys. Rev. Lett. 50, 1827 (1983); Zheng Yuming, Commun. Theor. Phys. (Beijing) 3, 31 (1984).

[4]A. Faessler, F. Fernandez, G. Lübeck, and K. Shimizu, Phys. Lett. 122B, 201 (1982); Nucl. Phys. A402, 555 (1983); A. Faessler and F. Fernandez, Phys. Lett. 124B, 145 (1983).

[5]D. Gromes and I. O. Stamatescu, Nucl. Phys. B112, 213 (1976).

[6]K. Maltmann and N. Isgur, Phys. Rev. Lett. 50, 1827 (1983).

[7]M. Harvey and J. Letourneux, Nucl. Phys. A424, 419 (1984).

[8]A. W. Hendry and D. B. Lichtenberg, Fortschr. Phys. 33, 139 (1985).

[9]C. J. Horowitz, E. J. Moniz, and J. W. Negele, Phys. Rev. D 31, 1689 (1985).

[10]M. Oka, Phys. Rev. D 31, 2274 (1985).

[11]M. Oka and C. J. Horowitz, Phys. Rev. D 31, 2773 (1985).

[12]F. Lenz, J. T. Londergan, E. J. Moniz, R. Rosenfelder, M. Stingl, and K. Yazaki, Ann. Phys. (N.Y.) 170, 65 (1986).

[13]D. Blaschke, F. Reinholz, G. Röpke, and D. Kremp, Dubna Report No. E2-84-572, 1984 (unpublished); Phys. Lett. 151B, 439 (1985).

[14]L. P. Kadanoff and G. Baym, Quantum Statistical Mechanics (Benjamin, New York, 1962); A. L. Fetter and J. D. Walecka, Quantum Theory of Many Particle Systems (McGraw-Hill, New York, 1971).

[15]G. Röpke, L. Münchow, and H. Schulz, Nucl. Phys. A379, 536 (1982); G. Röpke, M. Schmidt, L. Münchow, and H. Schulz, ibid. A399, 587 (1983).

[16]M. H. Storm and A. Watt, J. Phys. G 11, 217 (1985).

[17]M. Oka and K. Yazaki, Phys. Lett. 90B, 41 (1980).

[18]D. Vautherin and D. M. Brink, Phys. Rev. C 5, 626 (1972).

[19]G. Röpke, D. Blaschke, and H. Schulz, Phys. Lett. 174B, 5 (1986).

[20]H. Schulz, L. Münchow, G. Röpke, and M. Schmidt, Phys. Lett. **119B**, 12 (1982); H. Schulz, B. Kämpfer, H . W. Barz, G. Röpke, and J. Bondorf, *ibid*. **147B**, 15 (1984); H. Reinhardt and H. Schulz, Nucl. Phys. **A432**, 630 (1985).

[21]J. Kuti, J. Polonyi, and K. Szlachanyi, Phys. Lett. **98B**, 199 (1981); F. Karsh and H. Satz, Phys. Rev. D **21**, 1168 (1979); **22**, 480 (1980); J. Kapusta, Nucl. Phys. **B148**, 461 (1979); S.

A. Chin, Phys. Lett. **78B**, 552 (1978); H. Reinhardt, B. V. Dang, and H. Schulz, *ibid*. **159B**, 161 (1985).

[22]H. Satz, Nucl. Phys. **A418**, 447 (1984).

[23]See, e.g., Sec. 3 of the report by E. V. Shuryak and the references therein concerning QCD-motivated string models, Phys. Rep. **61**, 71 (1980).

[24]C. J. Horowitz, Phys. Lett. **162B**, 25 (1985).